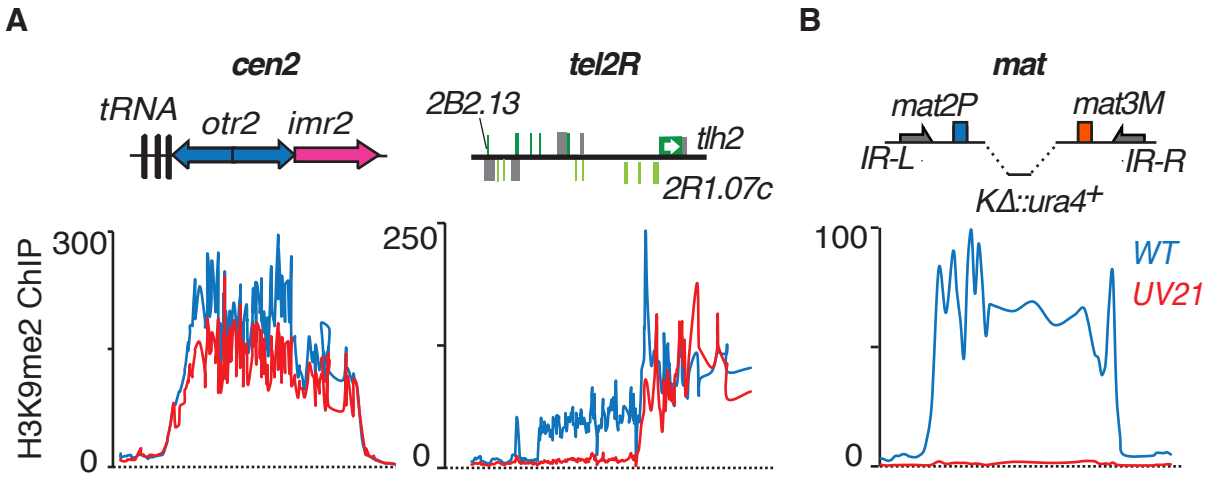

Figure S1. Loss of Heterochromatin at *KΔ::ura4*$^{+}$ in *UV21*, Related to Figure 1
(A and B) ChIP-chip analysis of H3K9me2 distribution at heterochromatic regions is shown for wild type and *UV21* strains. Note that the *UV21* mutant shows a complete loss of heterochromatin at *KΔ::ura4*$^{+}$ and considerable defects at telomeres, whereas centromeres are mostly unaffected.

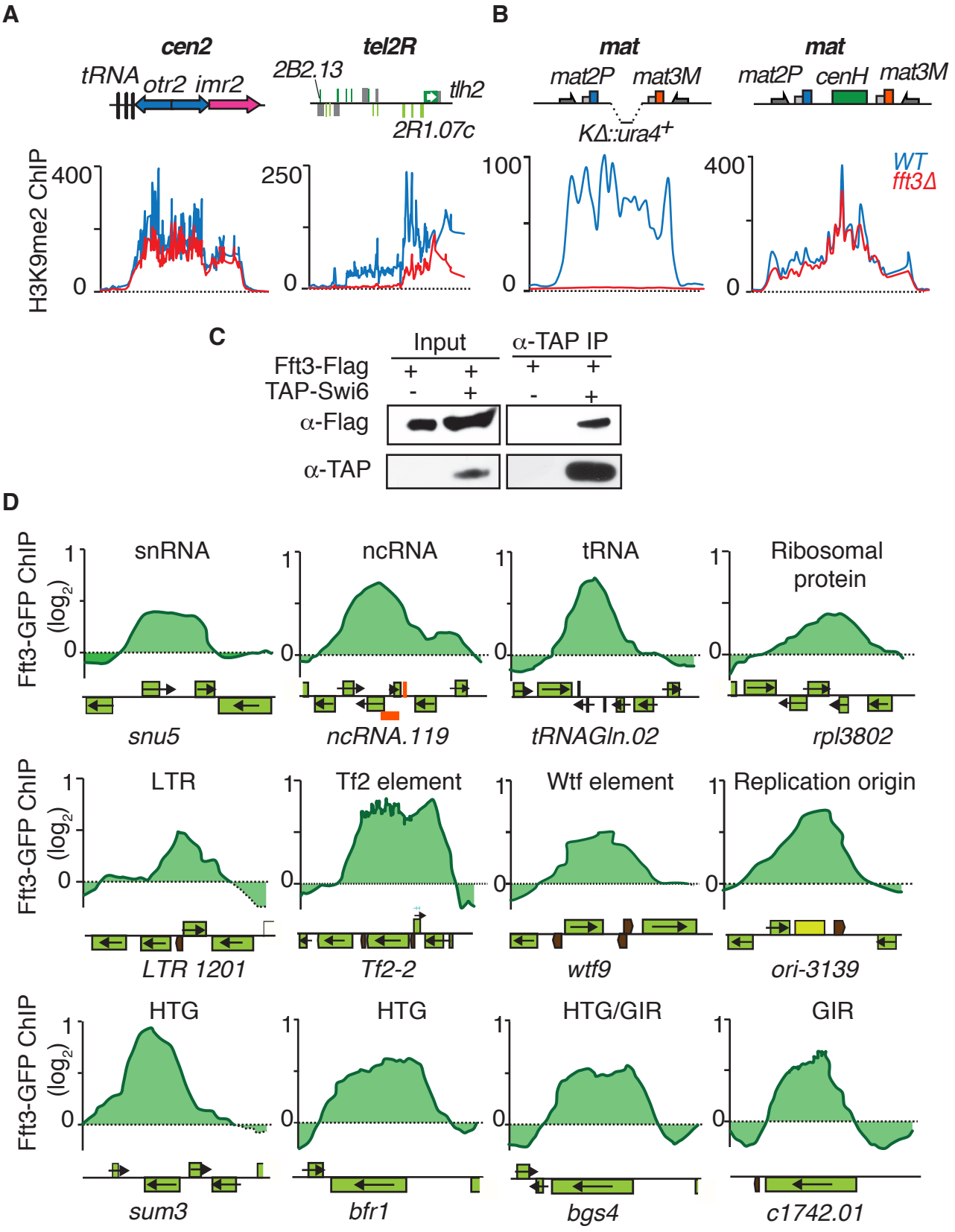

Figure S2. *fft3*Δ Phenocopies the Heterochromatin Defects of *UV21*, Related to Figure 2
(A and B) ChIP-chip analysis of H3K9me2 distribution at heterochromatic regions is shown for wild type and *fft3*Δ strains. (C) Fft3 interacts with heterochromatin factors. Co-immunoprecipitation analysis of the interaction between Fft3 and Swi6 is shown. (D) Fft3 localizes to various euchromatic loci. ChIP-chip analysis of Fft3-GFP distribution at the indicated loci is shown. HTG or GIR stands for highly transcribed gene or gene containing short internal repeats, respectively.

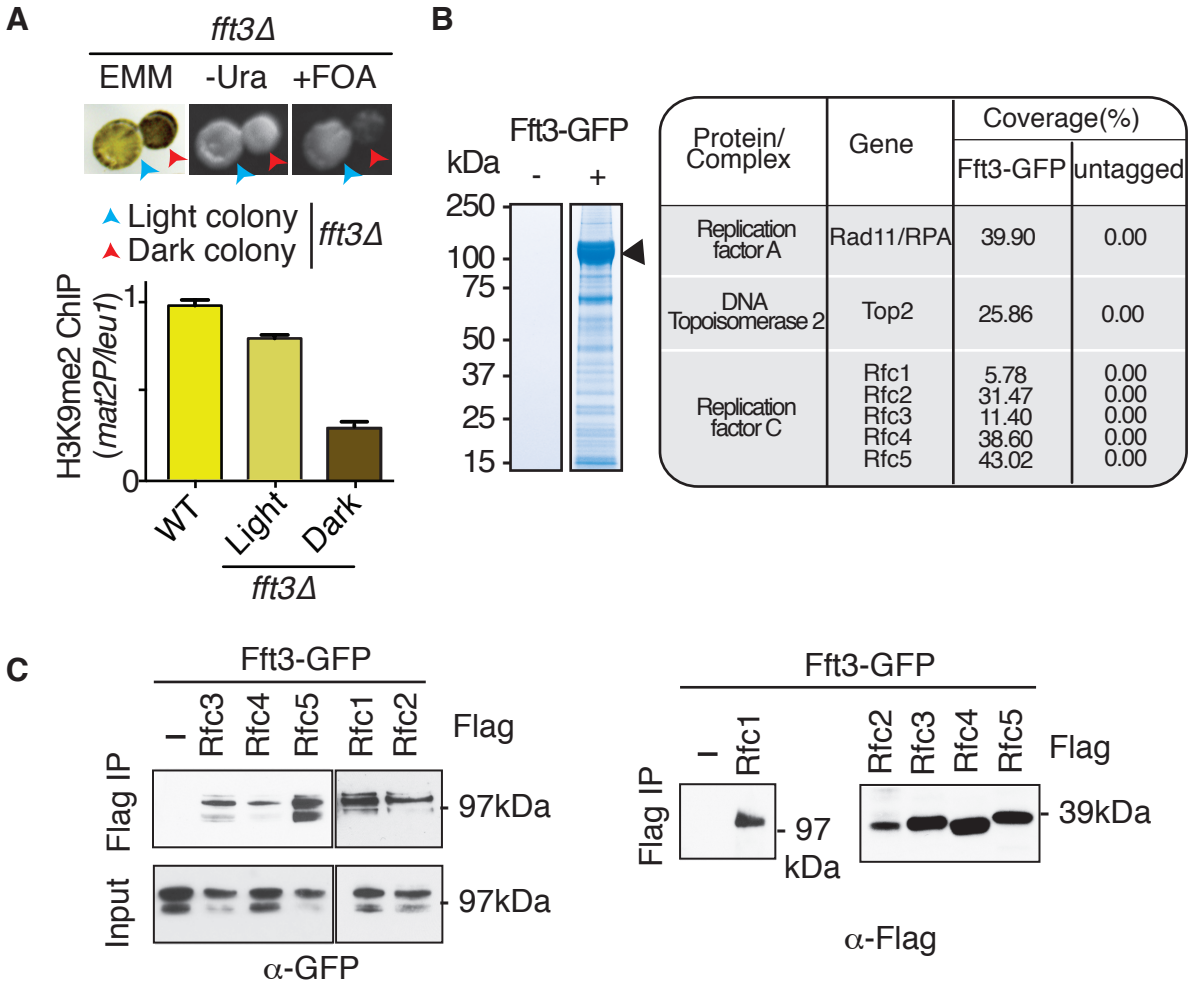

Figure S3. Fft3 Interacts with RFC, Related to Figure 3

(A) Analysis of H3K9me in *fft3*Δ. Two colonies representing the variegated phenotype of *fft3*Δ are shown in the top panel. Iodine staining yields light and dark colonies on EMM plates. Growth of light and dark stained colonies on media lacking uracil (-Ura) or media containing FOA (+FOA) is shown. Note that loss of *ura4*$^{+}$ silencing corresponds with the dark iodine staining due to haploid meiosis, and reduced H3K9me2 enrichment at *mat2P* relative to the control *leu1* locus as determined by ChIP-qPCR (bottom panel). The wild type value was set to 1. Error bars represent SD (n = 2). (B) Purification of Fft3-GFP from S phase cells. Cells were arrested using the *cdc25-22* allele at the G2/M boundary and released to grow synchronously until mid-S phase. Extracts from the untagged or Fft3-GFP strains were purified on anti-GFP agarose beads and the purification was visualized on an SDS-PAGE gel by CBB staining (left). Mass spectrometry data showing total peptide coverage (%) of the identified proteins is shown (right). (C) Co-immunoprecipitation (Co-IP) of Fft3-GFP with Flag-tagged RFC subunits. Cell extracts from the indicated strains were subjected to immunoprecipitation using anti-Flag antibody followed by western blotting. Detection of RFC subunits in anti-Flag IPed fractions is shown as control.

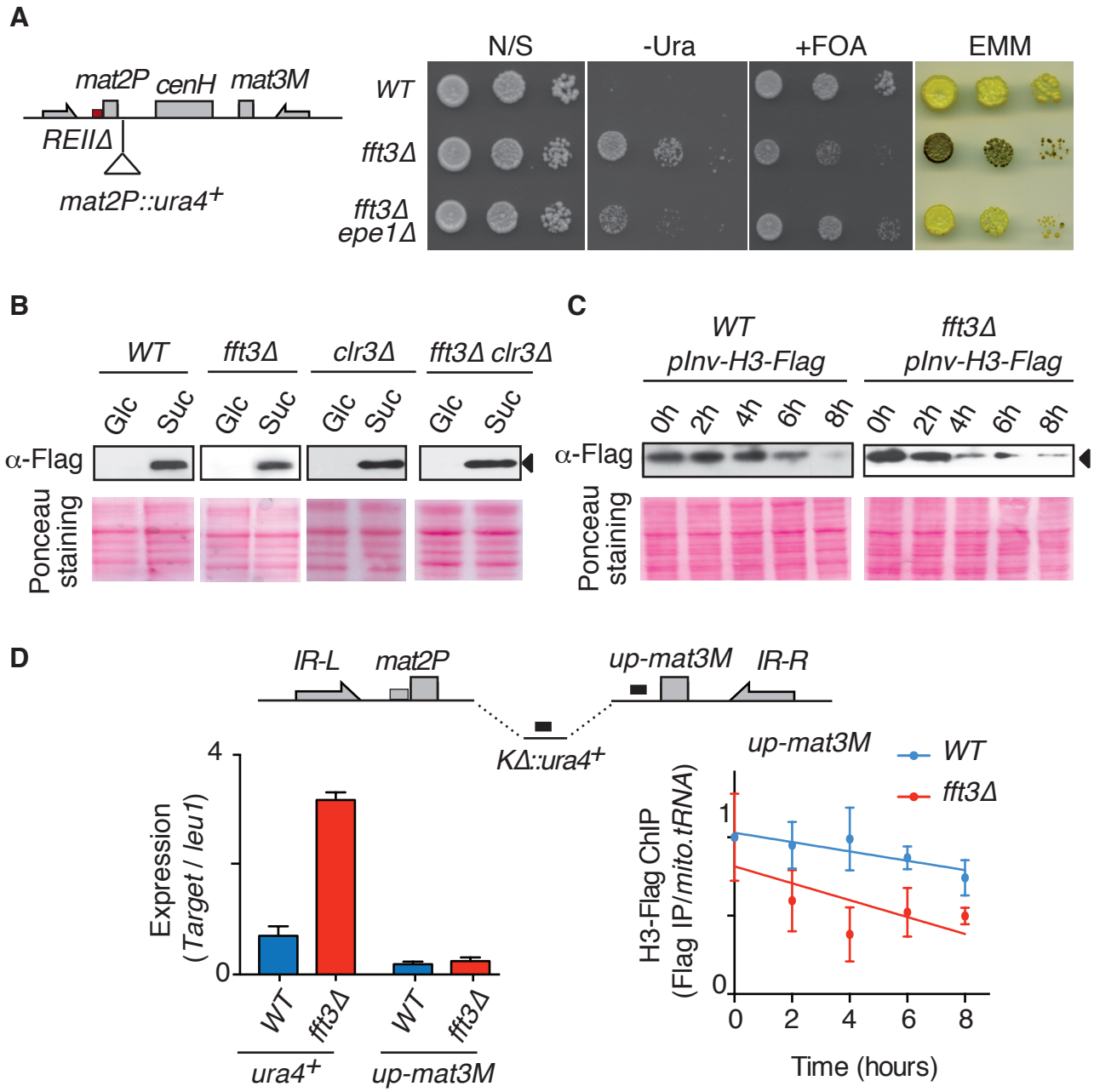

Figure S4. Fft3 affects histone turonver at the heterochromatic *mat* region, Related to Figure 4

(A) Loss of Epe1 rescues the *fft3*Δ silencing defect. Serial dilutions and iodine staining of the indicated strains are shown. (B) Western blot analysis of H3-Flag expression upon a switch in growth medium from glucose (Glc) to sucrose (Suc) for 2h (top). The Ponceau S staining is shown as a control for protein loading (bottom). (C) The expression of H3-Flag was monitored in extracts prepared from cells 0h, 2h, 4h, 6h and 8h after shifting to growth medium containing glucose (top). The Ponceau S staining is shown as a control for protein loading (bottom). (D) Loss of H3-Flag in *fft3*Δ at the transcriptionally inert region of the *mat* locus. Bottom left, the relative expression of indicated targets over *leu1* was determined by qRT-PCR in the indicated strains and are shown as the mean + SD (n=3). Bottom right, the H3-Flag fold enrichment relative to mitochondrial *tRNA* was determined by ChIP-qPCR for wild type (blue line) and *fft3*Δ (red line) and is shown as the mean ± SD (n=3). The 0 hour value was set to 1 for comparison between different time points. The location of regions used for qPCR are indicated by black boxes.

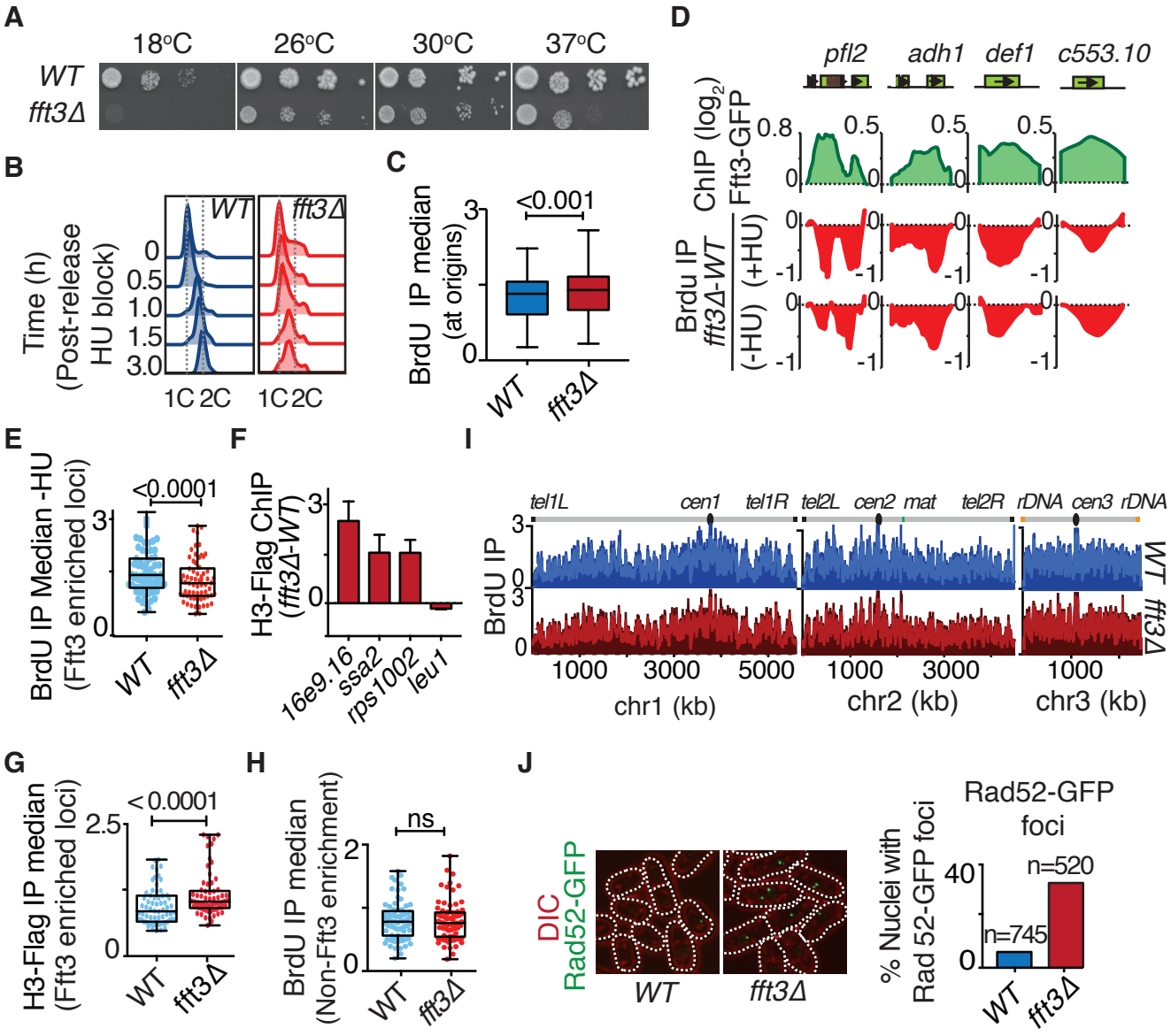

Figure S5. *fft3*Δ Cells Show Growth and Replication Defects, Related to Figure 5

(A) Serial dilutions of indicated strains on non-selective medium. (B) Cells were arrested by HU treatment for 4h and were collected upon release at the indicated time points for flow cytometry analysis. (C) The median of total BrdU incorporation at all origins, determined using ChIP-chip. (D) BrdU incorporation in the presence or absence of HU in *fft3*Δ for the indicated regions showing Fft3 enrichment. Signals were normalized to wild type. (E) The median of total BrdU incorporation in the absence of HU at 67 loci (see Table S1) showing Fft3 enrichment. (F) ChIP-qPCR analysis of H3-Flag incorporation at loci with (*16e9.16c, ssa2* and *rps1002*) or without (*leu1*) Fft3-GFP enrichment in *fft3*Δ. (G) The median of the total H3-Flag incorporation at 67 loci enriched for Fft3. The corresponding differences between the two strains are highly significant, *t*-test ($p<0.0001$). (H) The median of total BrdU incorporation at loci not enriched with Fft3. The corresponding differences between the two indicated strains are not statistically significant, *t*-test ($p = 0.87$ or ns). (I) ChIP-chip analysis of BrdU incorporation in wild type and *fft3*Δ showing the overall replication pattern. (J) *fft3*Δ accumulates DNA breaks as indicated by Rad52-GFP foci.

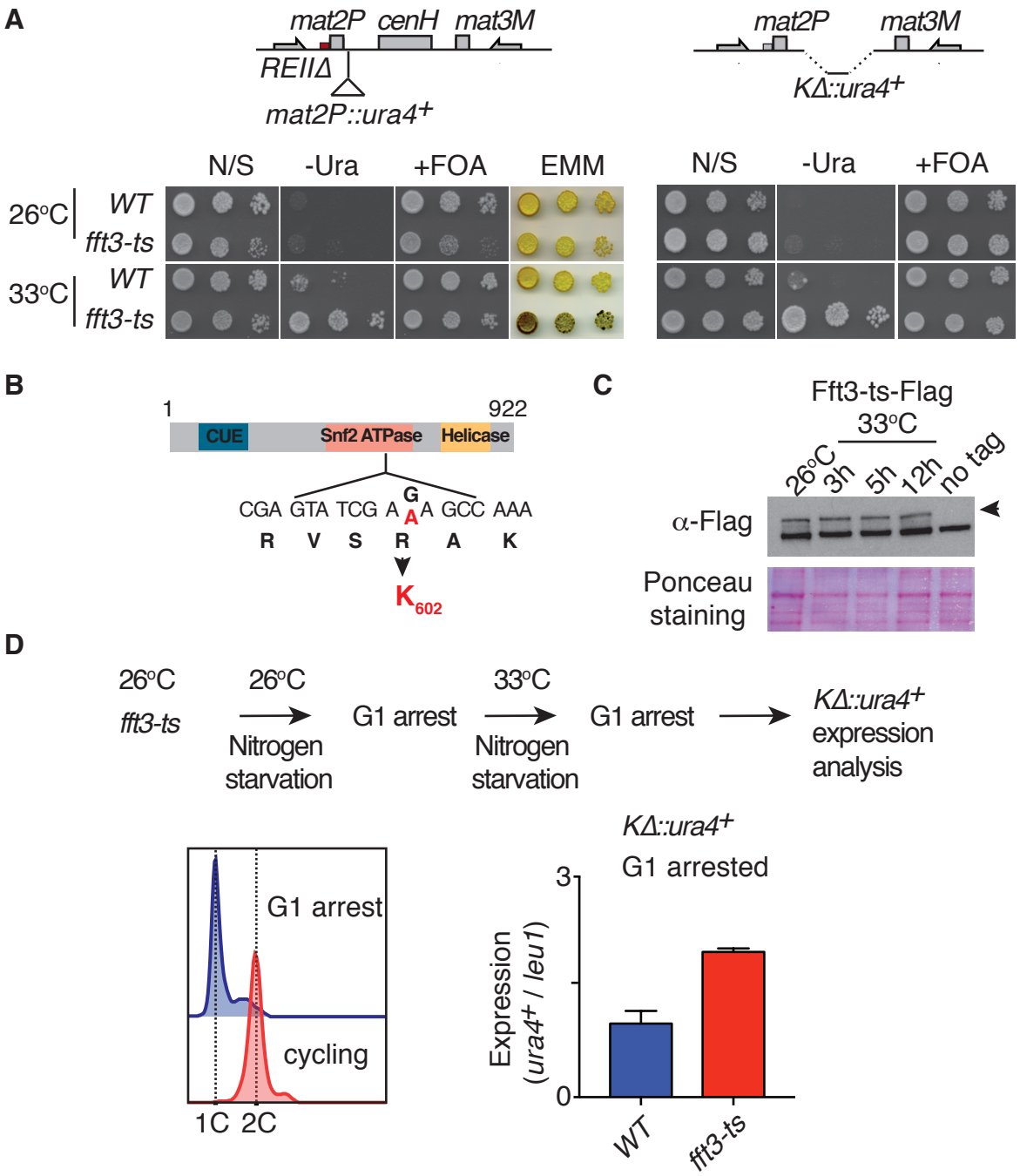

Figure S6. *fft3-ts* Cells Show Silencing Defects, Related to Figure 5

(A) Serial dilutions of wild type and *fft3-ts* cells were spotted onto non-selective media and incubated at the indicated temperatures for growth analysis. (B) Schematic representation showing the position of the point mutation associated with *fft3-ts*. (C) Western blot analysis of the Fft3-ts-Flag protein expression at the indicated temperatures. (D) Schematic depiction of the experimental design to investigate heterochromatin silencing without progression through S-phase (top). Flow cytometry analysis of cells arrested in G1 by nitrogen depletion. *1C* and *2C* refer to DNA content before and after DNA replication, respectively. Transcript levels of *KΔ::ura4+* relative to *leu1* in wild type (blue bars) and *fft3-ts* (red bars) were determined by qRT-PCR are shown as the mean + SD (n=2).

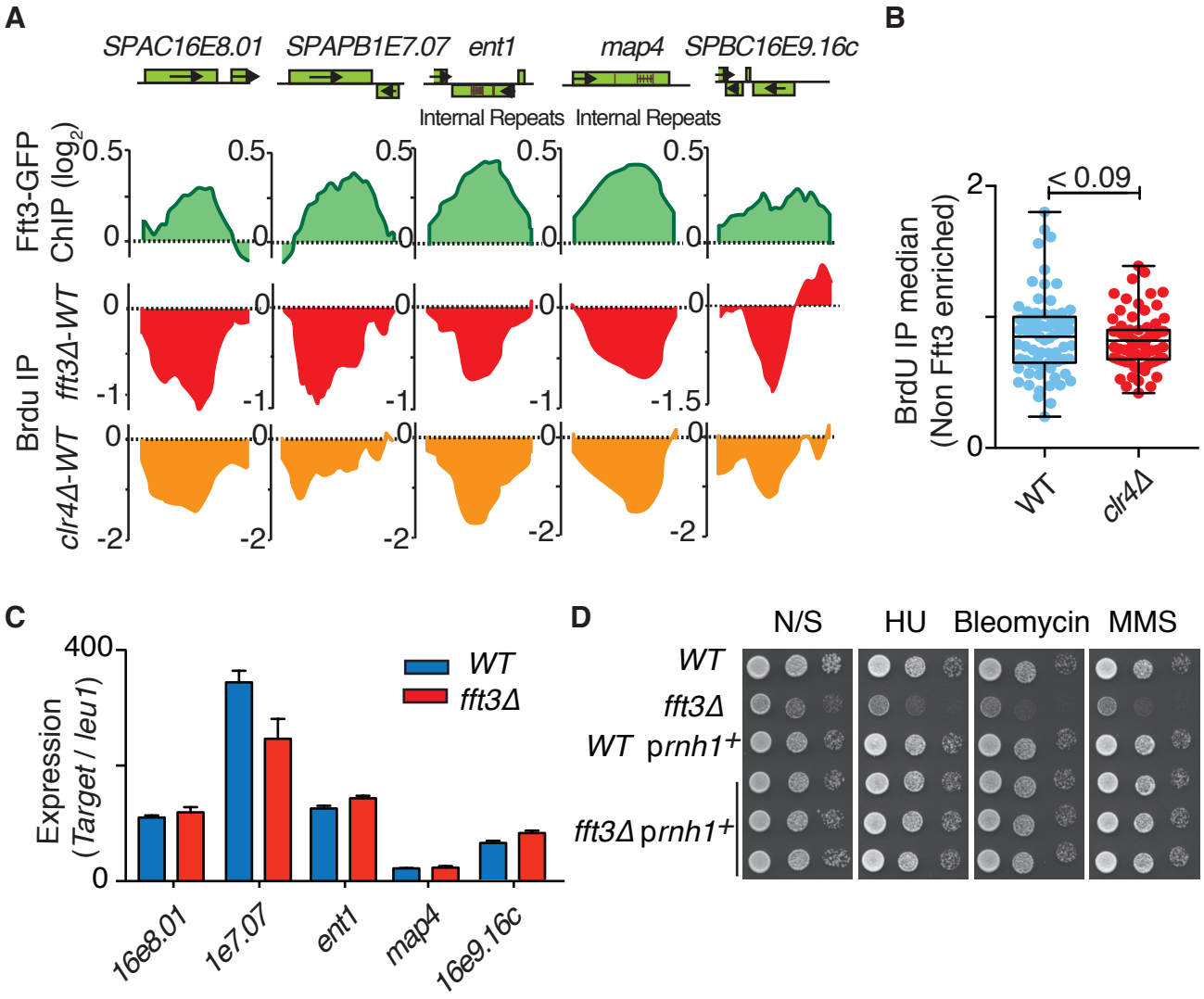

Figure S7. Replication Defects in *fft3*Δ and *clr4*Δ at Loci Enriched with Fft3-GFP, Related to Figure 6

(A) BrdU incorporation in *fft3*Δ and *clr4*Δ was determined by microarray analysis and is shown for the indicated regions enriched with Fft3-GFP. Signals were normalized to wild type. The distribution of Fft3-GFP determined by microarray analysis is shown on top. The locations of internal repeats are marked within the ORF of the indicated loci. (B) The median of total BrdU incorporation at loci not enriched with Fft3-GFP, as determined using ChIP-chip data from wild type and *clr4*Δ, is shown as a box plot. The corresponding differences between the strains are not highly significant, as determined by *t*-test ($p < 0.09$). (C) The expression of the indicated targets relative to *leu1* was determined by qRT-PCR and is shown as the mean + SD (n=3). (D) Growth defects and genotoxin sensitivity of *fft3*Δ are suppressed upon RNase H overexpression. Three independent isolates of *fft3*Δ transformed with plasmid containing Rnh1, encoding RNase H, are shown. Plates were incubated at 26 °C for 5 days.

List of Supplemental Tables: